

Ionospheric F2-Region Characteristics of Profile Parameters at an Equatorial Station During Low Solar Activity



*¹Ehinlafa, E. O., ²Àlàgbé, G. A., ¹Johnson, M. J., ¹Ige, S. O. and ³Adeniyi, J. O.

¹Department of Physics, University of Ilorin, Ilorin, Nigeria

²Department of Pure & Applied Physics, Ladoko Akintola University of Technology, Ogbomosho, Nigeria

³Private Individual, Pipeline Road, Ilorin, Nigeria

*Corresponding author's email: segunolu74@gmail.com Phone: +2348034343563

ORC-ID: 0009-0008-3982-8274

ABSTRACT

The ionospheric characteristics of the F2 region critical frequency (f_oF2), peak electron density (N_mF2) and the height of occurrence of electron density (h_mF2), was investigated over Ilorin (lat. 8.31°N, long. 4.34°E, dip lat. 2.95°), a station along the equatorial ionization anomaly trough, during a period of low solar activity (LSA). Diurnally, f_oF2 , N_mF2 and h_mF2 were found to have two characteristic peaks: pre-noon and post-noon peaks, except h_mF2 that has post-sunset peak. The f_oF2 and N_mF2 pre-noon peaks occurred around 0800–0900 LT, h_mF2 's peak around 1000 LT. The post-noon peaks of f_oF2 and N_mF2 were observed around 1500 and 1800 LT, while h_mF2 was observed around 1800 and 1900 LT. In general, the magnitude of the pre-noon peak is less than that of the post-noon/post-sunset peak for all the parameters, for all the seasons. The highest magnitudes of f_oF2 and N_mF2 were reached in the equinoctial months. The rapid faster electron drift in h_mF2 away from the equator is responsible for the sharp drop in f_oF2 and N_mF2 after sunset in all seasons. Seasonal peaks in general are suspected to be controlled by the enhanced $E \times B$ drifts and, the atmospheric wind, which is consistent with some earlier results obtained at some stations in the African region during low solar activity periods.

Keywords:

f_oF2 ,
 N_mF2 ,
 h_mF2 ,
Pre-noon peak,
Post-noon peak,
Post-sunset peak,
Equator anomaly,
Low Solar Activity.

INTRODUCTION

The F2 region is the most important region in the ionosphere because it is used for long range radio frequency communications. Variations in the ionospheric parameters associated with the F2-layer, namely, the critical frequency (f_oF2), the peak electron density (N_mF2) and the height of occurrence of peak electron density (h_mF2), mirror the behaviour of the F2 region ionosphere.

Observations show that the ionospheric parameters (f_oF2 , N_mF2 and h_mF2) increase in magnitude after sunrise; these increases occur more frequently at low latitudes. The maximum value is attained in the early afternoon and plummets just after sunset. The ionospheric parameters (f_oF2 , N_mF2 and h_mF2) usually attain their highest values near the equator.

The equatorial ionization anomaly, characterized by the occurrence of a trough in the ionization concentration at the equator and crests at about 17° in magnetic latitude in each hemisphere, has been thought to arise from the electrodynamic at the equator. Tidal oscillations in the

lower ionosphere move plasma across the magnetic field lines which are horizontal at the magnetic equator. The resulting E-region dynamo sets up an intense current sheet referred to as the equatorial electrojet (Anderson *et al.*, 2002; Babatunde *et al.*, 2017). These dynamo electric fields are transmitted along the dipole magnetic field lines to F region altitudes, where the uplift of ionization takes place. The zonal current flows eastward during the day and westward at night. Since an electric field is established perpendicular to the magnetic field, an $E \times B$ thrust moves the ionization vertically upwards during the day and downwards at night. This upward motion of ionization during the day is referred to as the equatorial fountain, since ionization rises above the magnetic equator until pressure forces become appreciable that it slows down and under the force of gravity moves along the field lines and is deposited at higher tropical latitudes.

For a better understanding of the ionospheric parameters, such as, f_oF2 spread, N_mF2 variation patterns and h_mF2 characteristics, several works have

been carried out. Lastovcka, *et al.* (2008), Oladipo *et al.* (2008), Atac *et al.* (2009) and Adebesein (2013 a and b) investigated the representation of ionospheric behavioural patterns as relate to the origin and estimating the long term trend in f_oF2 , variability of N_mF2 , and F2 layer characteristics in h_mF2 at different seasons, times of day, solar cycles, and latitudes.

Concerning the characteristics of the F2 region ionosphere, Ouattara and Zerbo (2011); Bilitza *et al.* (2014); Tariku (2015); Sawadogo *et al.* (2019) and Diabaté *et al.* (2019) highlighted the characteristics of the profiles of the ionospheric parameters (f_oF2 , N_mF2 and h_mF2) during various seasons, day, time, solar events, and latitude. Àlàgbé (2012) and Ouattara (2013) reported the variation of these ionospheric parameters during geomagnetically disturbed as well as quiet periods, for an equatorial station. Bai *et al.* (2020) combined the entropy weight method to develop the f_oF2 prediction model and provided reliable long-term predictions. A support vector machine model was utilized to establish an empirical local ionospheric forecasting model to predict f_oF2 (Chen *et al.*, 2010). Similarly, Olga Maltseva (2021) utilized the total electron content (TEC) to estimate f_oF2 and demonstrated the results for three stations in the southern hemisphere.

The present work used data from Ilorin (latitude 8.31°N, longitude 4.34°E, dip lat. 2.95°), Nigeria, to investigate the diurnal, seasonal and annual variation of f_oF2 , N_mF2 and h_mF2 , during low solar activity period. Some earlier works (e.g., Radicella and Adeniyi 1999; Anderson *et al.* 2006; Oladipo *et al.* 2009) adopted the idea of using representative months for each of the seasons and their results are reasonable and well documented.

MATERIALS AND METHODS

The data used consists of ionospheric F2 region parameters like the critical frequency (f_oF2), peak electron density (N_mF2) and the height of peak electron density (h_mF2). For f_oF2 and h_mF2 , the hourly values for a 10-day quiet period were taken over Ilorin (latitude 8.31 N, longitude 4.34 E, dip lat. 2.95°), an equatorial station in Nigeria, West Africa. The study is for the year 2010, a period of low solar activity (LSA). The datasets for f_oF2 and h_mF2 were obtained from the Digital Ionogram DataBase (DIDBase), and the ionograms were manually edited through the SAO Explorer software package.

The digisonde sounds the ionosphere every 15 minutes but this time interval is too small to reveal the changes desired for study. Therefore, an hourly interval resolution data of F2 region parameters for f_oF2 and h_mF2 was used for the study. This approach revealed noticeable changes in F2 region. The N_mF2 values were derived from the f_oF2 data using the relation in equation (1):

$$N_mF2 = 1.24 \times 10^{10} \cdot (f_oF2)^2 \quad (1)$$

where N_mF2 is given in m^{-3} and f_oF2 in MHz.

For the seasonal pattern of the f_oF2 and h_mF2 , data for the months of April, July, October and November were used to represent Spring, Summer, Autumn and Winter, respectively. Each set of data covers the entire 24 hours of the day for each of the four representative months of the year 2010. For the annual pattern, we used the average monthly values across each hour.

RESULTS AND DISCUSSIONS

Ionospheric f_oF2 Observations

Figure 1 represents the average seasonal variation of the critical frequency (f_oF2) over Ilorin, during the low solar activity (LSA) year of 2010. In general, f_oF2 increases from sunrise around 0500 LT and reaches its first peak (pre-noon peak) around 0800–0900 LT for all seasons. The least f_oF2 first peak (7.7 MHz) was observed in Summer season while the greatest peak (8.3 MHz) was observed in Spring around 0800–0900 LT, during this period of solar activity. Thereafter, there is a general daytime reduction in f_oF2 , reaching a minimum between 1000 and 1200 LT for the all the seasons. The least depression occurred in Spring around 1000 LT, while the greatest depression occurred in Summer at about 1100LT, during the low solar activity.

Around local noon, the F2 region ionosphere had reached a dynamic stability with respect to losses by recombination, and production by solar radiation according (Fejer, 1997). It is observed that f_oF2 increases after sunrise; the increase being more prominent at lower latitudes. The maximum value of f_oF2 was attained in the early afternoon, followed by a rapid decrease shortly after sunset. A second peak (the post-noon peak) occurred between 1500 and 1800 LT for all seasons. During the solar epoch considered, the magnitude of the post-noon peak was the least in Summer (7.3 MHz) and the highest peak was observed in Spring (9.7 MHz) at the time interval 1500LT-1800LT, during this period of solar activity. The two f_oF2 peaks observed are ascribed to abrupt electron density gradients triggered by the onset and turn-off of solar ionization, as well as the superimposition of Spread-F on the background electron density (Chou and Lee 2008, Adebesein *et al.*, 2012).

Concerning the night-time variation of f_oF2 (1800–0500 LT), a general sharp drop in the value of f_oF2 became noticeable immediately after sunset for the all the seasons. This decay began around 1800 LT, and continued until around 0500 LT, at which time a pre-sunrise minimum occurred. For this night-time event, the critical frequency is lowest in Winter. Both the observed pre-noon and afternoon f_oF2 peaks in the F2-region variation are ascribed to variations of vertical $E \times B$ plasma drifts (Fejer *et al.* 1999; Adebesein *et al.* 2013a).

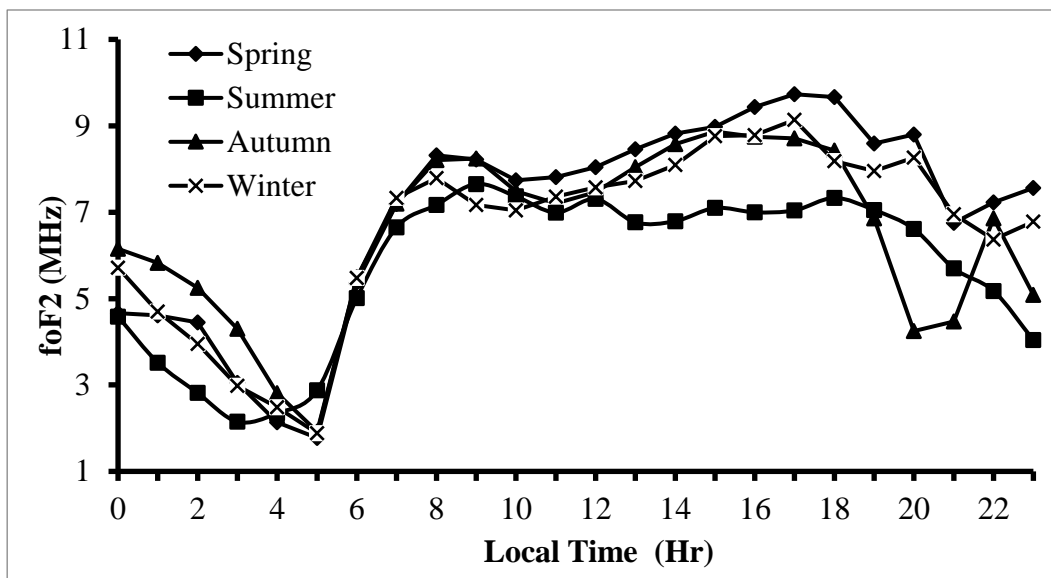


Figure 1: Diurnal variation of f_oF_2 for all seasons over Ilorin during period of low solar activity

The average hourly annual plot of f_oF_2 variation against local time (LT) is represented in figure 2. During the LSA period, an annual average f_oF_2 magnitude of 7.9 MHz was observed around 0800 LT for the pre-noon peak and its post-noon peak value of 8.7 MHz occurred at about 1700 LT. An annual average daytime reduction in f_oF_2 , reaching a minimum was observed between

1000 and 1100 LT for all the seasons. Annually, the nighttime variation decayed sharply during all the seasons until f_oF_2 increases from around 0500 LT. This observation is in total agreement with the results obtained for Ouagadougou (12.4°N, 1.5°E; dip 5.9°), during a low solar activity period (Adeniyi *et al.* 2007; Àlàgbé, 2012)5

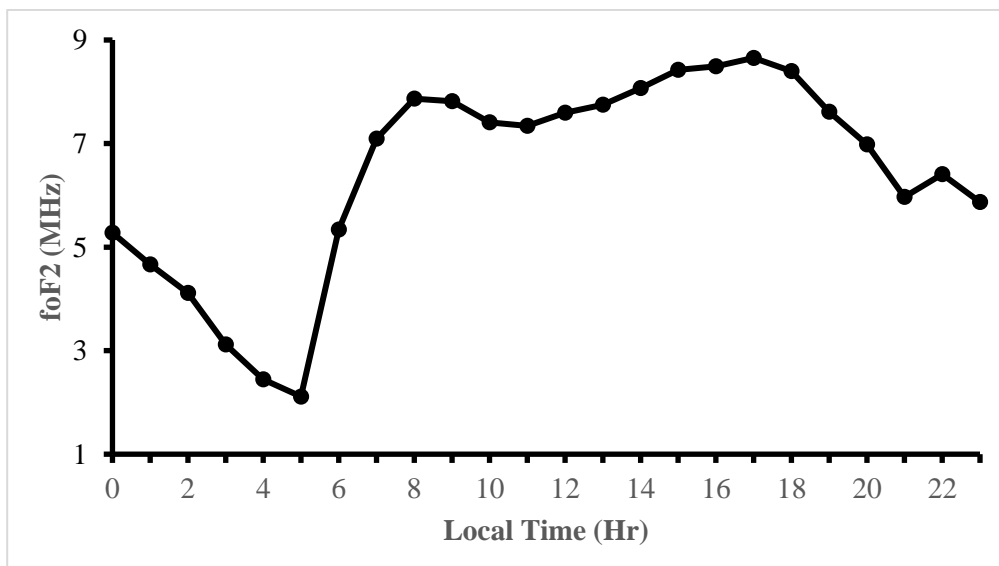


Figure 2: Hourly average annual variation of f_oF_2 during low solar activity period

Variation Patterns of Peak electron density (N_mF_2)

Figure 3 highlights the average seasonal variation of the peak electron density (N_mF_2) over Ilorin, during low solar activity. N_mF_2 increases from sunrise around 0500 LT and reaches a pre-noon peak of $(7.3\text{--}8.6) \times 10^{11} \text{ m}^{-3}$ around 0800–0900 LT for all the seasons. The least pre-noon peak of electron density was observed in Summer

$(7.3 \times 10^{11} \text{ m}^{-3})$, followed by the Winter $(7.5 \times 10^{11} \text{ m}^{-3})$, then the Autumn $(8.4 \times 10^{11} \text{ m}^{-3})$; the greatest pre-noon peak of electron density occurred in Spring $(8.6 \times 10^{11} \text{ m}^{-3})$. Thereafter, there is a general daytime reduction in electron density, creating a trough and reaching a minimum between 1000 LT and 1100 LT. The least depression occurred in Spring, while the

greatest depression occurred in Summer. Around noon time, the N_mF2 has been shown to attain a production enhancement by solar radiation and dynamical stability with recombination losses. N_mF2 increases after sunrise, a phenomenon which is more prominent at lower latitudes (Fejer, 1995). The maximum value of N_mF2 is attained early in the afternoon and a rapid decrease occurred shortly after sunset. A post-noon peak was observed between 1500 and 1800 LT for all the seasons. The peak electron density attained the highest value during the equinoctial months, especially in Spring ($11.7 \times 10^{11} / m^3$) around 1800 LT and the lowest value in the solstitial months, especially in Summer ($6.7 \times$

$10^{11} / m^3$) around 1800 LT. These observations are in agreement with the results obtained for Ouagadougou ($12.4^\circ N, 1.5^\circ E$; dip 5.9°) by other workers, during a low solar activity period (Radicella and Adeniyi, 1999; Oladipo *et al.*, 2009; Sawadogo *et al.*, 2019). At nighttime (1800–0500 LT), a general sharp drop in N_mF2 occurred immediately after sunset. This sharp drop was observed around 1800 LT. This decay progressed during all the seasons till around 0500 LT, at which time a pre-sunrise minimum occurred. The least value of electron density ($1.4 \times 10^{11} / m^3$) was attained in Summer and the highest during Spring ($7.2 \times 10^{11} / m^3$).

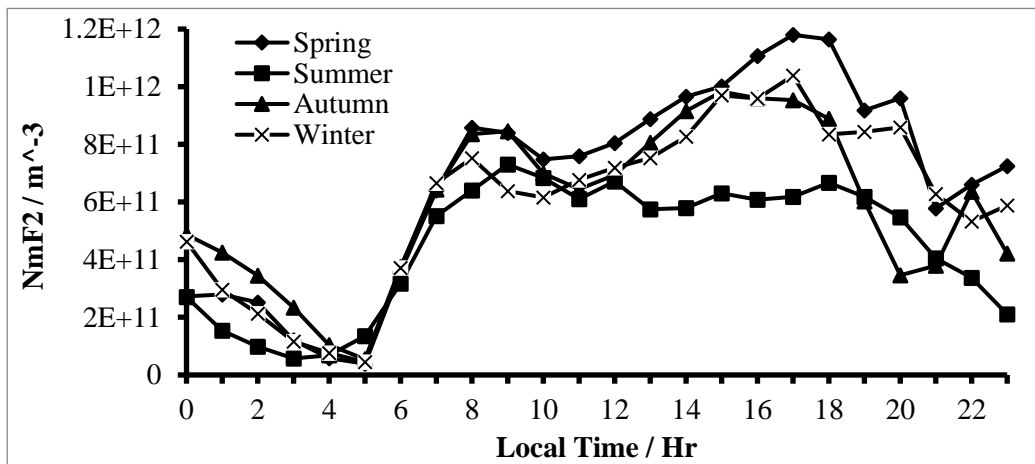


Figure 3: Hourly average diurnal peak electron density (N_mF2) over Ilorin for solar minimum period

Figure 4 depicts hourly average annual variation plot of peak electron density (N_mF2) during low solar activity. For this LSA period, N_mF2 displayed a post-noon peak

of an average magnitude of $9.5 \times 10^{11} / m^3$ around 1700LT, while the pre-noon peak with an average magnitude of $7.7 \times 10^{11} / m^3$ occurred around 0800 LT.

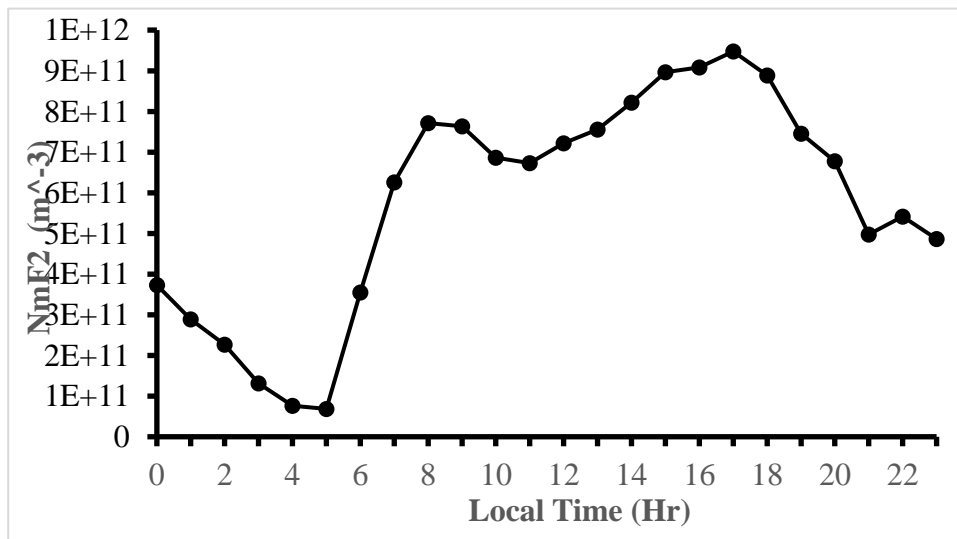


Figure 4: Annual average variation of Peak Electron Density (N_mF2) for all seasons over Ilorin

Seasonal h_mF_2 Observations

Depicted in figure 5 is the corresponding average seasonal height of the F_2 peak electron density. The h_mF_2 observations for all the seasons indicate a sharp and gradual rise within the sunrise period of 0600–1000 LT. During the daytime, there is a pre-noon peak around 1000 LT, ranging from 316 km to 353 km for all the seasons. The least h_mF_2 pre-noon peak was observed in Summer (316 km) and the highest h_mF_2 pre-noon peak of h_mF_2 in Spring (353 km), during this period of solar activity. It is believed that the stronger vertical $E \times B$ drift in equinoctial season moves the plasma to a higher altitude where the recombination loss becomes much weaker; the plasma in higher altitudes therefore has a longer lifetime, and then yield a higher magnitude in Spring (Chen *et al.*, 2008). Subsequently, between 1100LT and 1600 LT, h_mF_2 ranged from 310 km to 367 km within this period for all the seasons.

The second peak of h_mF_2 (post-sunset peak) occurred between 1600–1900 LT during all the seasons except during June solstice. During nighttime period, a post-sunset peak of h_mF_2 was recorded between 1800 and 1900 LT for all the seasons. However, the highest h_mF_2 magnitude was recorded in Winter (392 km) around 1800 LT and the least h_mF_2 magnitude was observed in

Summer (310 km) around 1900 LT. Adebessin *et al.* (2013a) suggested that the positive correlation between h_mF_2 and the F region vertical drift found during the nighttime between 1800 and 2100 LT could be helpful in representing the post-sunset peak of h_mF_2 around 1800 and 1900 LT. Immediately after this time, an abrupt decrease occurred in the seasonal patterns up till 0500 LT within a range of 245–320 km. The differences between the pre-noon peaks and the post-sunset peaks' magnitudes are not much pronounced except during the Winter.

The average peak height, h_mF_2 , profile for the entire 24 hours revealed that our result is in agreement with general theory that above 300 km, the apparent vertical velocity is about the same as the vertical $E \times B$ plasma drift (Bittencourt and Abdu, 1981). Hence, our result substantiates the fact that during daytime, the h_mF_2 shows rapid increase. The result further suggests that between 0900LT and 2100 LT, the general theory that vertical drifts obtained by digisonde measurements only matches the $E \times B$ drift if the F region is higher than 300 km, is reliable. However, this does not hold for the nighttime (2200–0600 LT) and early morning (0600–0900) periods in the present study, during low solar activity.

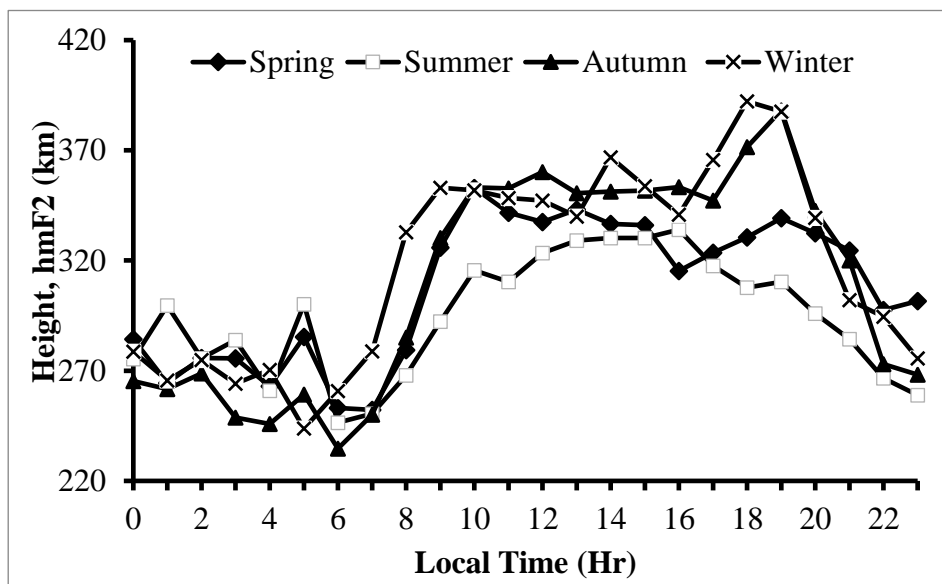


Figure 5: Hourly average seasonal height of the F_2 peak electron density during low solar activity

Figure 6 shows the average hourly annual height of the F_2 peak electron density. The post-sunset peak of an average magnitude 356 km occurred around 1900 LT; the pre-noon peak with an average magnitude of 343 km occurred around 1000 LT.

A trough in the daytime profile of h_mF_2 occurred between 1500LT and 1800 LT; h_mF_2 began to decrease

sharply at 1900 LT, reaching a pre-sunrise minimum at about 0600 LT. This was observed for all the seasons. This correlates with the daytime and nighttime patterns observed in f_oF_2 and in N_mF_2 . This is generally attributed to the vertical $E \times B$ drift mechanism causing the electrons to move away from the equator.

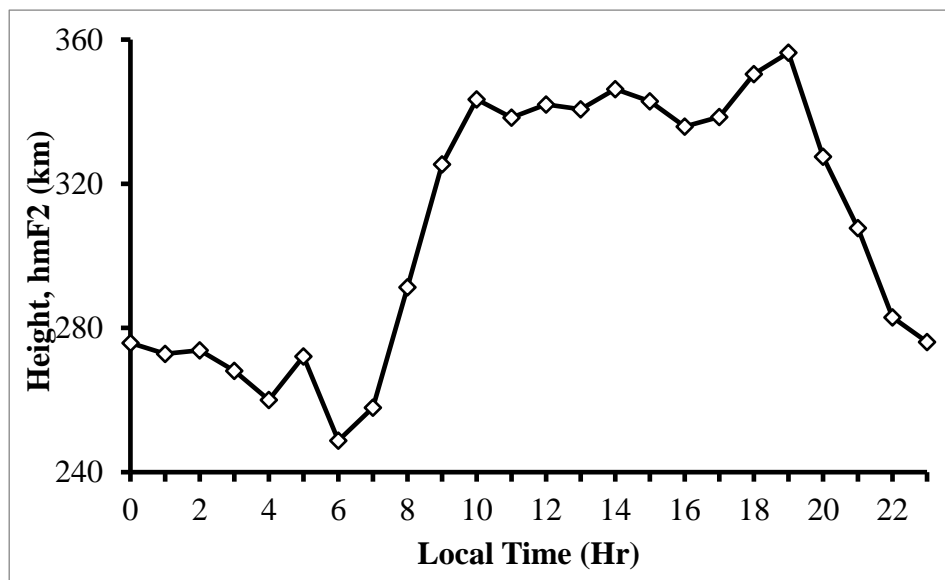


Figure 6: Hourly average annual height of the F2 peak electron density for Solar Minimum

CONCLUSION

In this study of ionospheric data from Ilorin, a station located along the equatorial ionization anomaly (EIA), the salient results of this work are presented as follows: The diurnal observation revealed that f_oF2 and N_mF2 are both more pronounced during the daytime (7.0–7.7 MHz) and $(7.3\text{--}7.5) \times 10^{11} \text{ m}^{-3}$ than the nighttime (2.5–7.6 MHz) and $(1.4\text{--}7.2) \times 10^{11} \text{ m}^{-3}$, respectively, having two characteristic peaks: pre-noon and post-noon peaks. The two characteristic peaks were ascribed to abrupt electron density gradients triggered by the onset and turn-off of solar ionization and superimposition of Spread-F on the background electron density. The ionospheric parameters f_oF2 and N_mF2 post-noon peaks magnitude are by a factor of 1.2 more than the pre-noon peaks for all seasons during this LSA period. The least magnitudes of f_oF2 variation were attained during the pre-noon peak between 0800 LT and 0900 LT with a magnitude range of (7.7–8.3 MHz). For this pre-noon peak, the highest was observed in Spring (8.3 MHz), followed by Autumn season (8.2 MHz), then winter (7.8 MHz) and the least in Summer (7.7 MHz). The post-noon peak was observed between 1500 and 1800 LT for all seasons. In all the seasons, the pre-noon peak is less than the post-sunset peak. Annually, the average pre-noon peak of 7.9 MHz magnitude was observed around 0800 LT while the post-noon peak was 8.7 MHz around 1700 LT for the LSA period. A h_mF2 pre-noon peak with a magnitude range of (316–353) km around 1000 LT during the daytime while during the nighttime, a post-sunset peak of h_mF2 with a magnitude range of (310–392) km between 1800 and 1900 LT was observed for all seasons during this period of LSA. The differences between the pre-noon peaks and the post-sunset peaks magnitudes are not much pronounced

except during the Winter. During nighttime, an observed enhancement in h_mF2 directly after sunset (fig. 5) is a pointer to the fact that ions are moved to a state of lower recombination coefficient and hence electron density should be sustained for an elongated period. However, this was not so, as a decrease in electron density was evident from our plots (figs. 1 and 3). This is because the influx of a post-sunset peak in upward plasma drift is indicative of sudden faster electron depletion from the equatorial ionosphere. Seasonal peaks in f_oF2 and N_mF2 as well as in h_mF2 are suspected to be controlled by the enhanced $E \times B$ drifts and atmospheric wind which agrees with the result of previous works.

ACKNOWLEDGEMENTS

This study was made possible by the data obtained from the Ilorin (latitude 8.31 N, longitude 4.34 E, dip lat. 2.95°) Digital Ionogram DataBase (DIDBase) online site. The authors appreciate Digisonde owners and international ionogram scaling teams for the good job done and for ensuring the availability of data to DIDBase online site for public use.

REFERENCES

- Adebesin, B.O., Adeniyi, J.O., Adimula, I.A., Reinisch, B.W., and Yumoto, K., (2013a) Equatorial vertical plasma drift velocities and electron densities inferred from ground-based ionosonde measurements during low solar activity; *J. Atmos. Sol. Terr. Phys.* **97**, 58–64, doi: [10.1016/j.jastp.2013.02.010](https://doi.org/10.1016/j.jastp.2013.02.010).
- Adebesin, B.O., Adeniyi, J.O., Adimula, I.A., Reinisch, B.W. and Yumoto, K. (2013b)

- F2 layer characteristics and electrojet strength over an Equatorial station; *Adv. Space Res.*, **52**(5), 791–800, doi: [10.1016/j.asr.2013.05.025](https://doi.org/10.1016/j.asr.2013.05.025)
- Adebesin, B.O. (2012) f_oF2 variations during geomagnetic disturbances at the rise of solar cycle 23; *Indian J. Radio and Space Phys.* **41**(3), 323–331
- Adeniyi, J.O., Oladipo, O.A. and Radicella, S.M. (2007) Variability of f_oF2 for an equatorial station and comparison with the f_oF2 maps in IRI model; *J. Atmos. Sol. Terr. Phys.* **69**, 721–733
- Àlàgbé, G.A. (2012) Geomagnetic storm effects on F2 layer peak electron density and other profile parameters at high solar activity at an equatorial station; *J. Phys. Sci. Innovation* **4**, 5–12, ISSN 2277–0119
- Anderson, D.N., Anghel, A., Yumoto, K., Ishitsuka, M., Kudeki, E., (2002) Estimating daytime, vertical E B drift velocities in the equatorial F region using ground-based magnetometer observations. *Geophys. Res. Lett.* **29** (12). <http://dx.doi.org/10.1029/2001GL014562>.
- Atac, A., Ozguc, A. and Pektas, R. (2009) The variability of f_oF2 in different phases of solar cycle 23; *J. Atmos. Sol. Terr. Phys.* **71**, 583–588.
- Babatunde, A., Olamike, R., Teiji, D.F., Nurul, U., Shazana, A.H., and Akimassa, Y. (2017) Longitudinal Variation of Equatorial Electrojet and the Occurrence of Its Counter Electrojet. *Annales Geophysicae*, **35**, 535–545.
- Bai, H., Feng, F., Wang, J. (2020) A Combination Prediction Model of Long-Term Ionospheric f_oF2 Based on Entropy Weight Method. *Entropy* **2020**, **22**, 442.
- Bilitza, D., Altadill, D., Zhang, Y., Mertens, C., Truhlik, V., Richards, P., McKinnell, L.A. and Reinisch, B. (2014) The International Reference Ionosphere 2012—A Model of International Collaboration. *Journal of Space Weather and Space Climate*, **4**, A07.
- Bittencourt, J.A. and Abdu, M.A. (1981) A theoretical comparison between apparent and real vertical ionization drift velocities in the equatorial F region. *J. Geophys. Res.*, **86**, 2451–2454.
- Chen, C.H., Liu, J.Y., Yumoto, K., Lin, C.H., Fang, T.W. (2008) Equatorial ionization anomaly of the total electron content and equatorial electrojet of ground-based geomagnetic field strength *J. Atmos. Sol. Terr. Phys.*, **70**, 2172–2183.
- Chen, C., Wu, Z.S., Xu, Z.W., Sun, S.J., Ding, Z.H., Ban, P.P. (2010) Forecasting the local ionospheric f_oF2 parameter 1 hour ahead during disturbed geomagnetic conditions. *J. Geophys. Res. Space Phys.* **2010**, **115**, 135–146.
- Chou Y.T. and Lee C.C. (2008) Ionospheric variability at Taiwan low latitude station: Comparison between observations and IRI 2001 model; *Adv. Space Res.* **42**, 673–681.
- Diabaté, A., Zerbo, J.-L. and Ouattara, F. (2019) Variation of the f_oF2 Parameter during Fluctuating Activity: Prediction with IRI-2012 Compared to Measured Data from Ouagadougou Ionosonde Station during Solar Cycles 21 and 22. *Vietnam Journal of Earth Sciences*, **41**, 69–78.
- Fejer, B.G., Scherliess, L., de Paula, E.R. (1999) Effects of the vertical plasma drift velocity on the generation and evolution of equatorial spread F. *J. Geophys. Res.*, **104**, 19854–19869.
- Fejer, B.G. (1997) The electrodynamics of the low latitude ionosphere recent results and future challenges; *J. Atmos. Sol. Terr. Phys.* **59**, 1465–1482.
- Fejer, B.G., de Paula, E.R., Heelis, R.A. and Hanson, W.B. (1995) Global equatorial ionosphere vertical plasma drifts measured by the AE-E Satellite; *J. Geophys. Res.* **100**, 5769–5776.
- Jayachandran, B., Balachandran, N.R., Balan, N. and Rao, P.B., (1995): Short time variability of the ionospheric electron content and peak electron density during solar cycles for a low latitude station, *J. Atmos. Sol. Terr. Phys.*, **52**, 1599–1605.
- Lastovcka, J., Yue, X. and Wan, W. (2008) Long-Term Trends in f_oF2 : Their Estimating and Origin. *Annales Geophysicae*, **26**, 593–598.
- Oladipo, O.A., Adeniyi, J.O., Radicella, S.M. and Obrou, O.K. (2008) Variability of equatorial ionospheric electron density at fixed heights below the F2 peak; *J. Atmos. Sol. Terr. Phys.* **70**, 1056–1065.
- Oladipo, O.A., Adeniyi, J.O., and Radicella, S.M. (2009) Electron density distribution at fixed heights N(h): Gaussian distribution test; *J. Atmos. Sol. Terr. Phys.* **71**, 1–10
- Olga, M., (2021) The Influence of Space Weather on the Relationship between the Parameters TEC and f_oF2 of the Ionosphere, *IEEE J. Radio Freq. Identify*, **5**, 261 - 268

Ouattara, F. (2013) IRI-2007 f_oF_2 Predictions at Ouagadougou Station during Quiet Time Periods from 1985 to 1995. Archives of Physics Research, 4, 12-18.

Ouattara, F. and Zerbo, J.L. (2011) Ouagadougou Station F2 Layer Parameters, Yearly and Seasonal Variations during Severe Geomagnetic Storms Generated by Coronal Mass Ejections (CMEs) and Fluctuating Wind Streams. International Journal of the Physical Sciences, 6, 4854-4860.

Radicella, S.M. and Adeniyi, J.O., (1999) Equatorial ionospheric electron density below the F2 peak. *Radio Science*, **34**(5), 1153- 1163.

Sawadogo, W.E., Zerbo, J.-L. and Ouattara, F. (2019) Diurnal Variation of F2-Layer Critical Frequency under Solar Activity Recurrent Conditions during Solar Cycles 21 and 22 at Ouagadougou Station: Prediction with IRI-2012. Scientific Research and Essays, 14, 111-118.

Tariku, Y.A. (2015) TEC Prediction Performance of the IRI-2012 Model over Ethiopia during the Rising Phase of Solar Cycle 24 (2009-2011). *Earth, Planets and Space*, 67, 140.